Electronic Supplementary Information (ESI)

Cytotoxic and apoptotic effects of ternary silver(I) complexes bearing 2-formylpyridine thiosemicarbazones and 1,10-phenanthroline

Débora E. S. Silva,[a] ✉ Amanda B. Becceneri,[b] Mariana C. Solcia,[c] João V. B. Santiago,[a] Mariete B. Moreira,[a] José A. Gomes Neto,[a] Fernando R. Pavan,[c] Márcia R. Cominetti,[b] José C. M. Pereira[a] and Adelino V. G. Netto[a] ✉

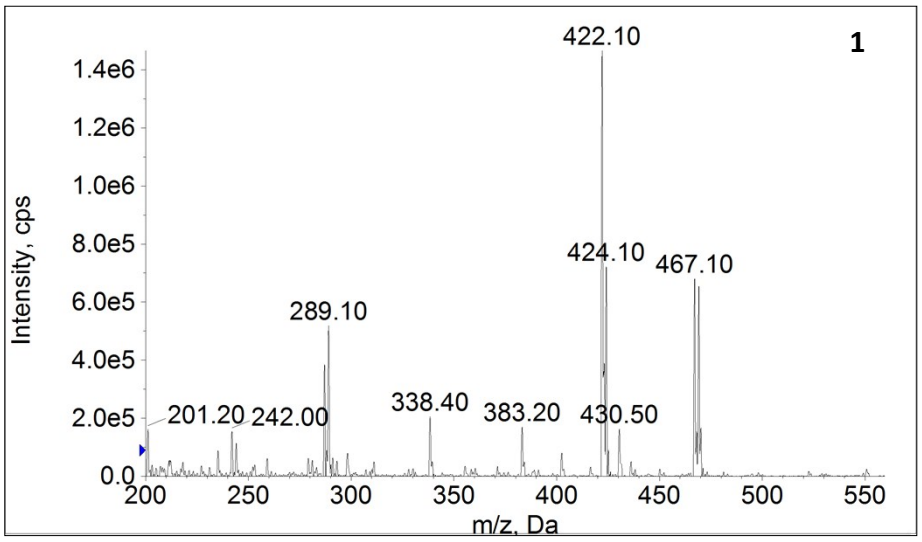

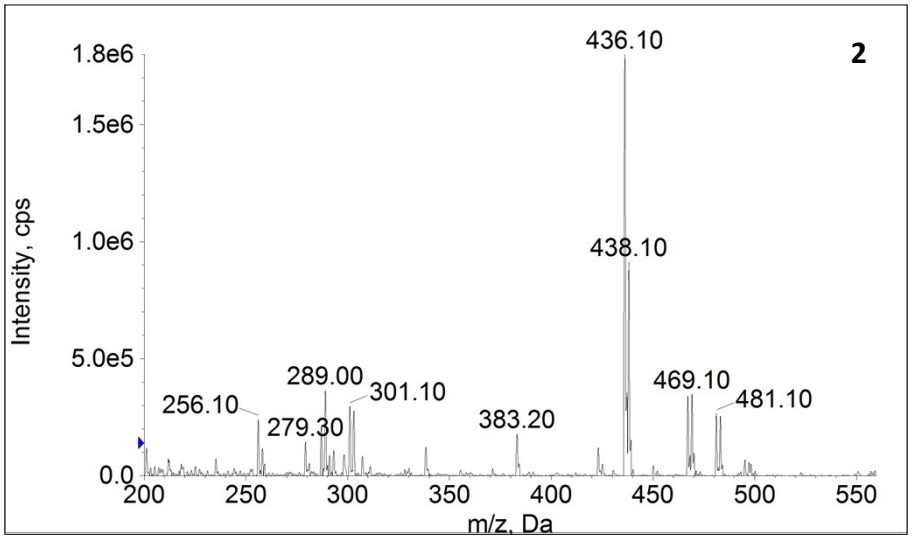

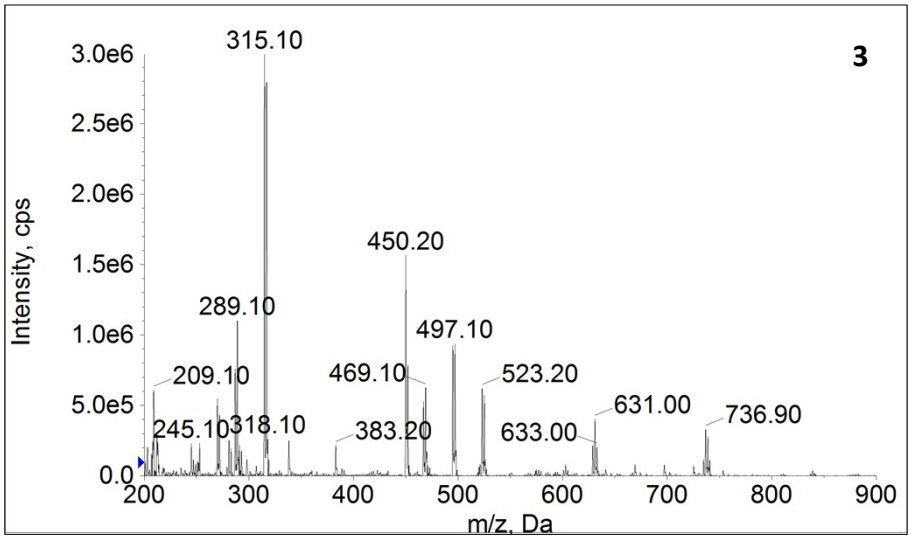

Fig. S1. ESI-MS spectra of compounds **1-3**.

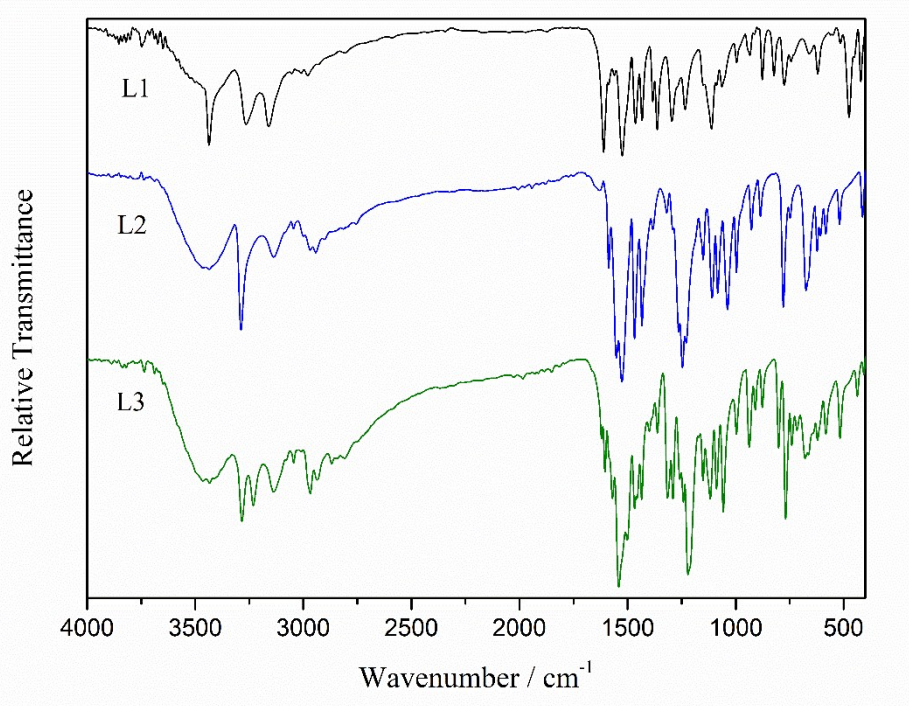

(A)

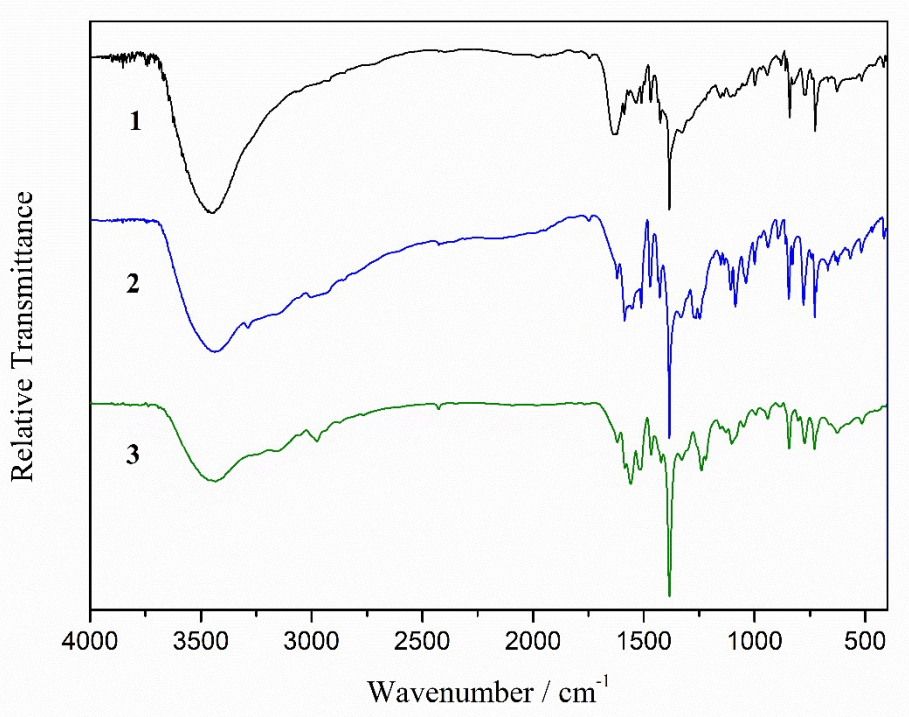

(B)

Fig. S2. IR spectra of ligands L1-L3 (A) and compounds **1-3** (B).

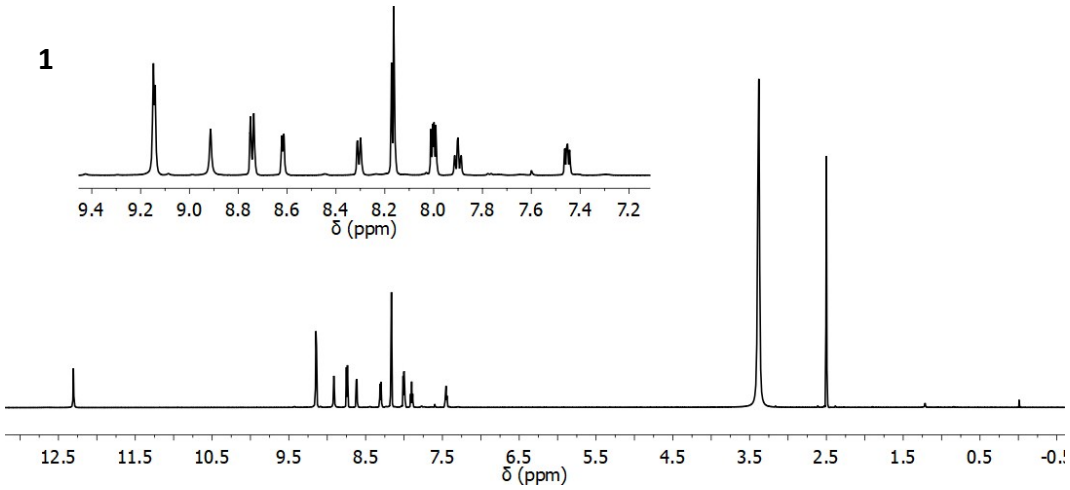

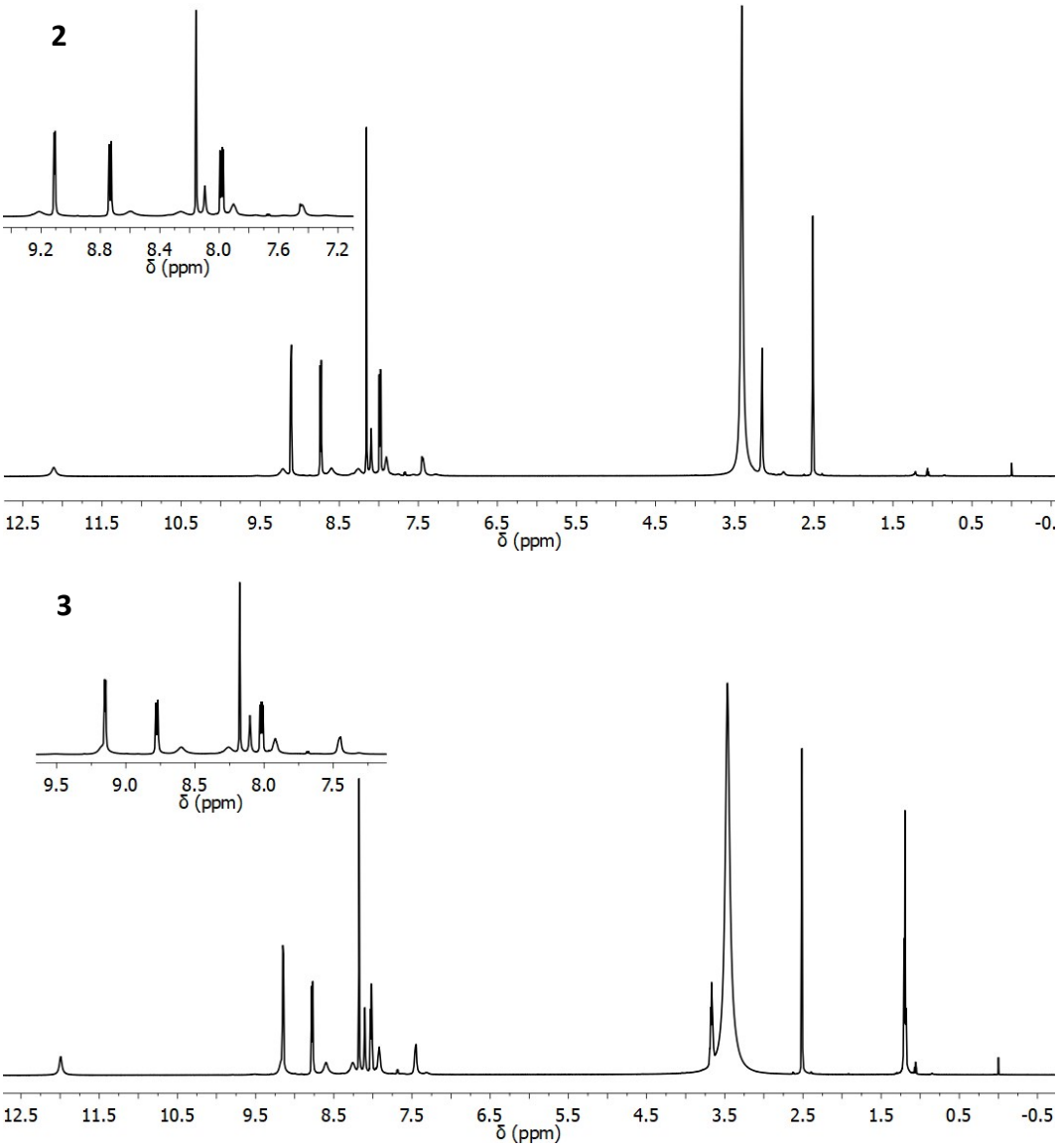

Fig. S3. ^{1}H NMR spectra of compounds **1-3** in DMSO-d_6.

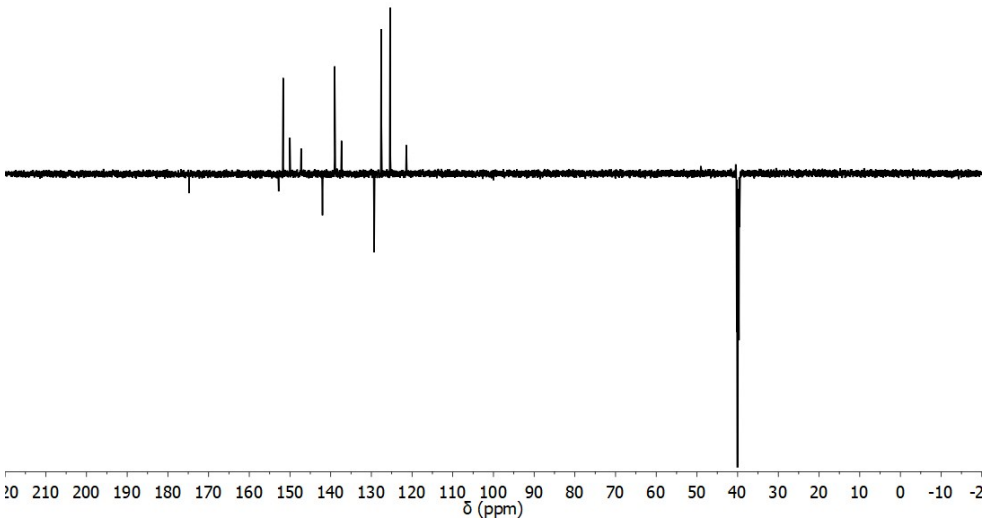

Fig. S4. ^{13}C-DEPTQ NMR spectrum of **1** in DMSO-d_6.

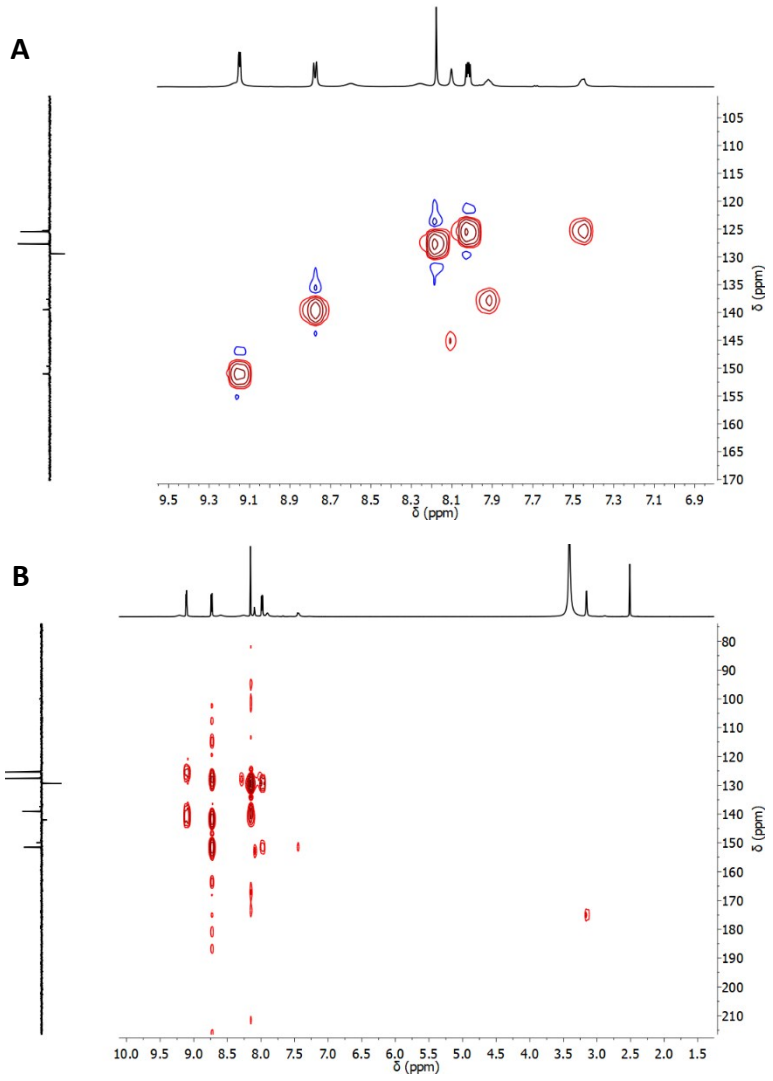

Fig. S5. ^{1}H-^{13}C HSQC and HMBC NMR spectra of **2** in DMSO-d_6.

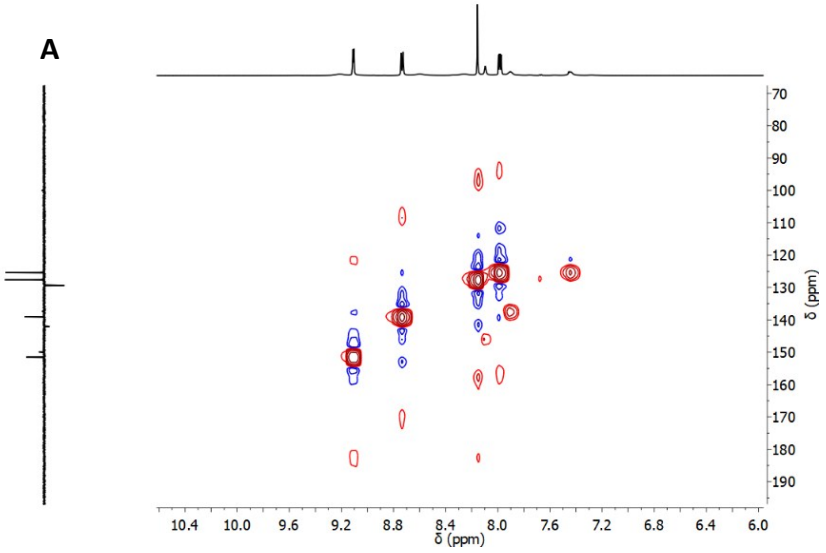

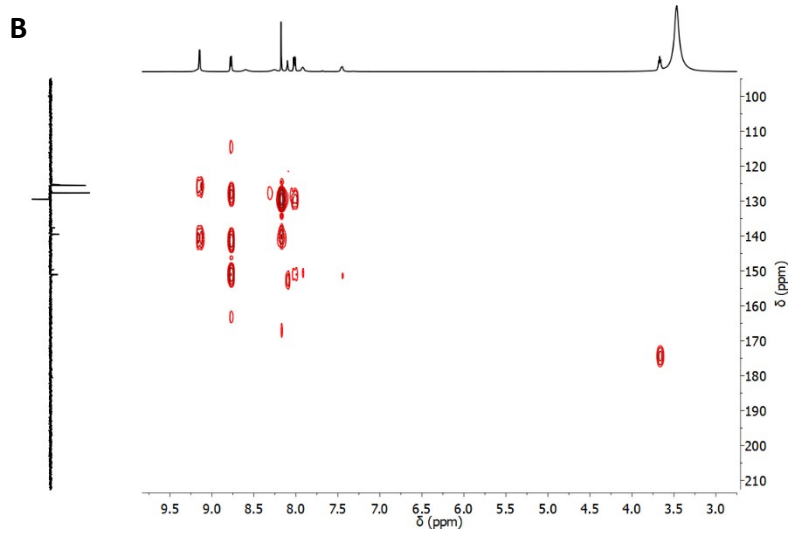

Fig. S6. ^{1}H-^{13}C HSQC and HMBC NMR spectra of **3** in DMSO-d_6.

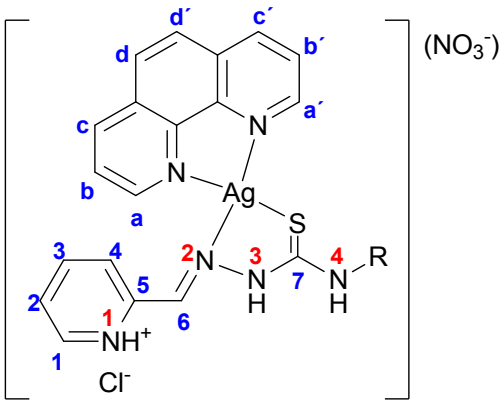

R = H (**1**); CH_3 (**2**) and CH_2CH_3 (**3**)

Fig. S7. Numbering scheme for NMR assignments of compounds.

Table S1. Selected ^{1}H and ^{13}C NMR chemical shifts for compounds L1-L3 and **1-3**.

NMR	**δ (ppm)**		
^{1}H	**1 (L1)**	**2 (L2)**	**3 (L3)**
^{3}NH	12.35 (11.80)	12.01 (11.70)	11.98 (11.75)
^{4}NH	9.16 (8.46) 8.93 (8.29)	9.20 (8.68)	9.14 (8.84)
^{13}C			
CS	174.35 (178.53)	175.18 (177.96)	174.10 (176.89)

CH=N	146.83 (139.67)	145.85 (141.96)	145.07 (139.94)

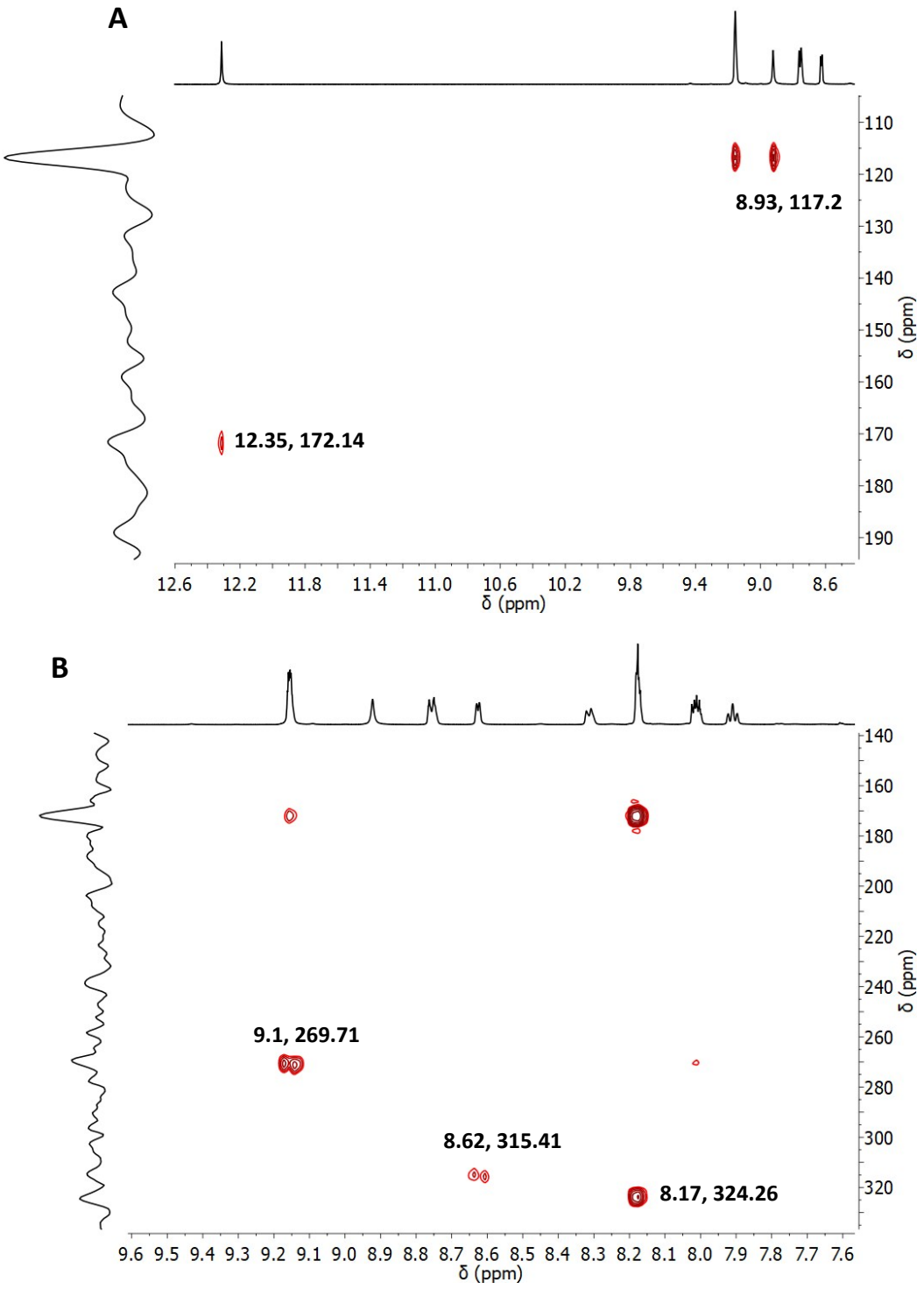

Fig. S8. ^{1}H-^{15}N HSQC (A) and HMBC (B) NMR spectra of compound **1** in DMSO-d_6.

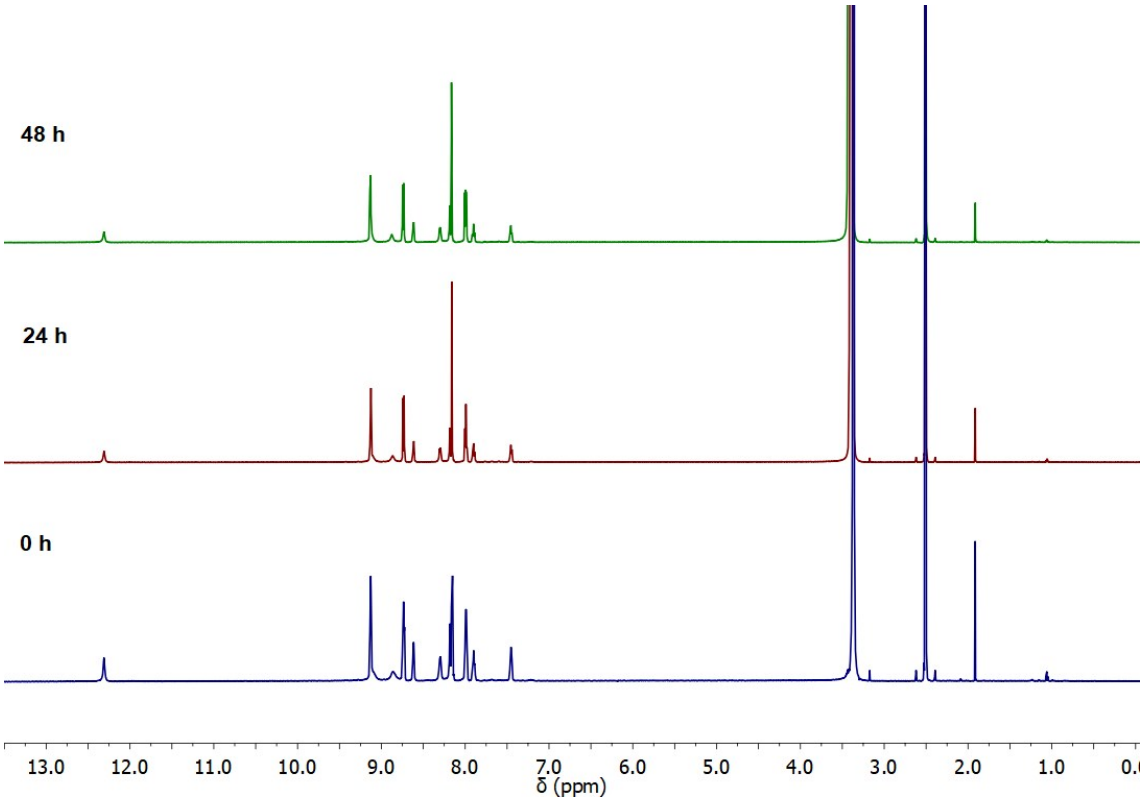
48 h
24 h
0 h
13.0
12.0
11.0
10.0
9.0
8.0
7.0
6.0
5.0
4.0
3.0
2.0
1.0
δ (ppm)

(A)

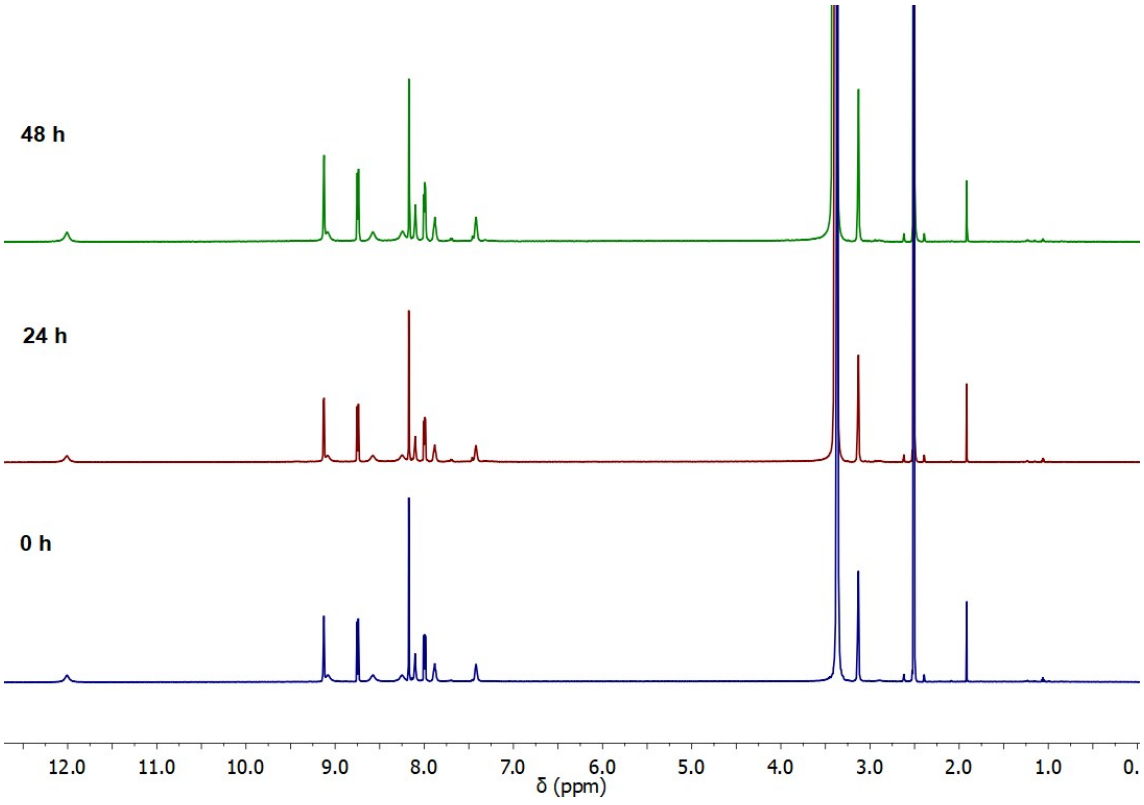
48 h
24 h
0 h
12.0
11.0
10.0
9.0
8.0
7.0
6.0
5.0
4.0
3.0
2.0
1.0
δ (ppm)

(B)

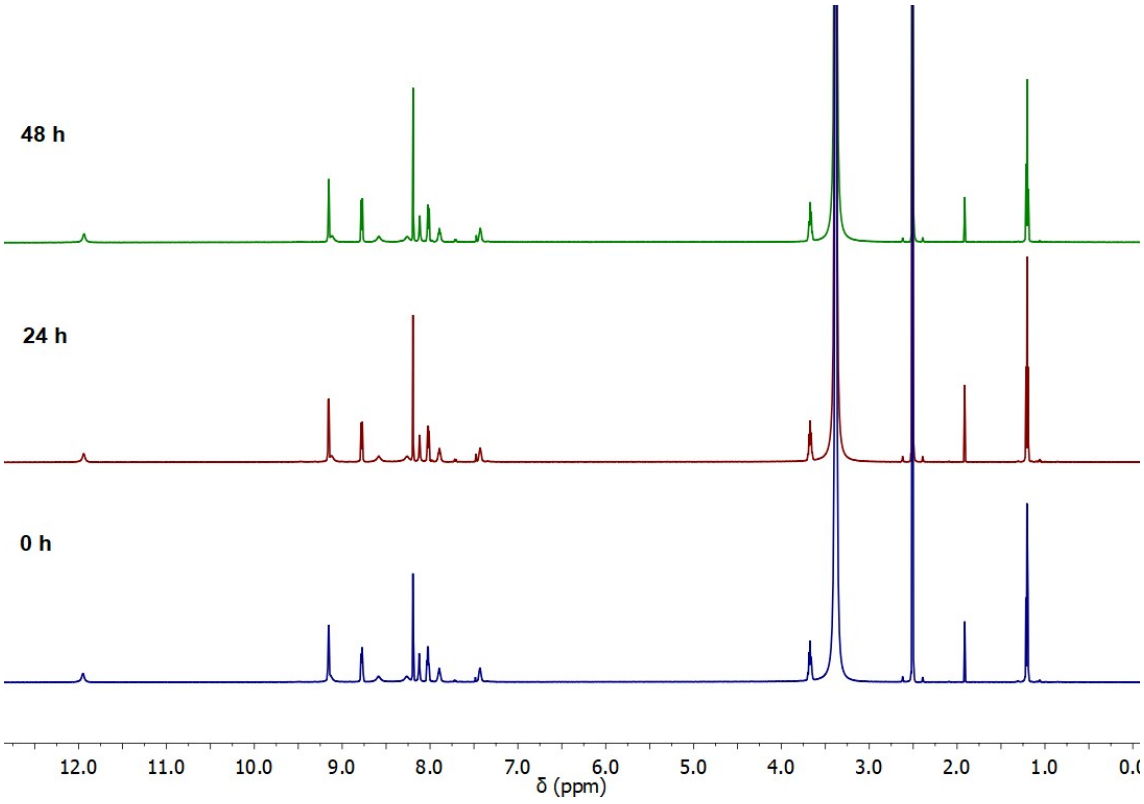

(C)

Fig. S9. ^{1}H NMR spectra of complexes (A) **1**, (B) **2** and (C) **3** recorded in DMSO-d_6 over a period of 48 hours.

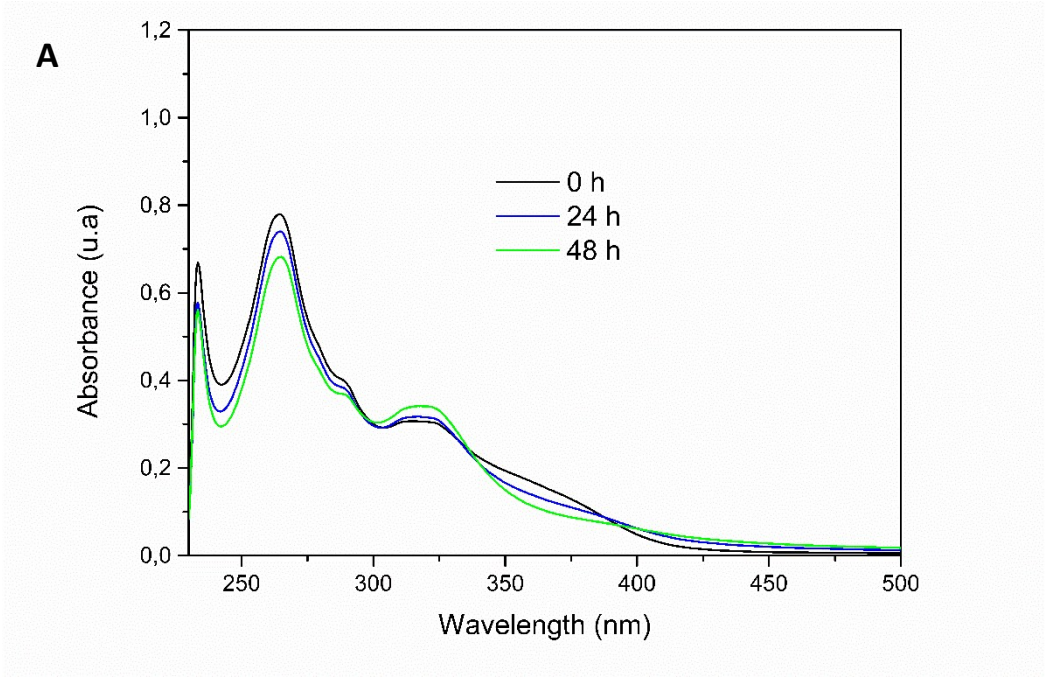

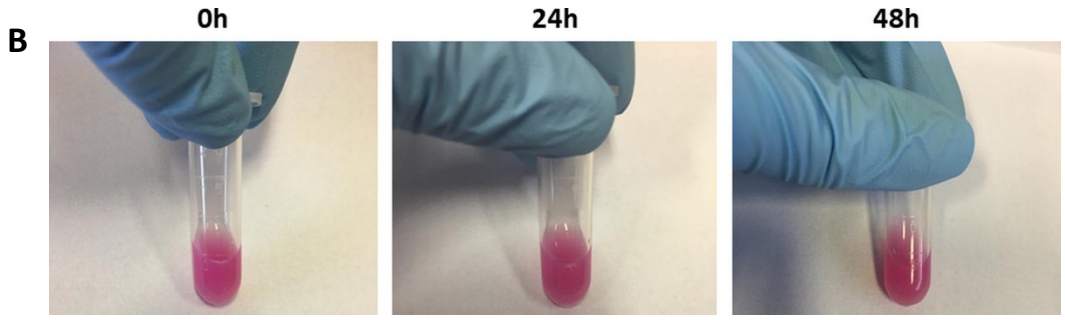

Fig. S10. Evaluation of stability of complex **1** in biological medium. **A)** UV-Vis spectrum of **1** recorded in Tris-HCl buffer (pH 7.4; 2% DMSO) over a period of 48 hours. **B)** Images recorded of a solution of **1** (1 mg mL^{-1}, 5% DMSO) in DMEM cell culture medium over a period of 48 hours.

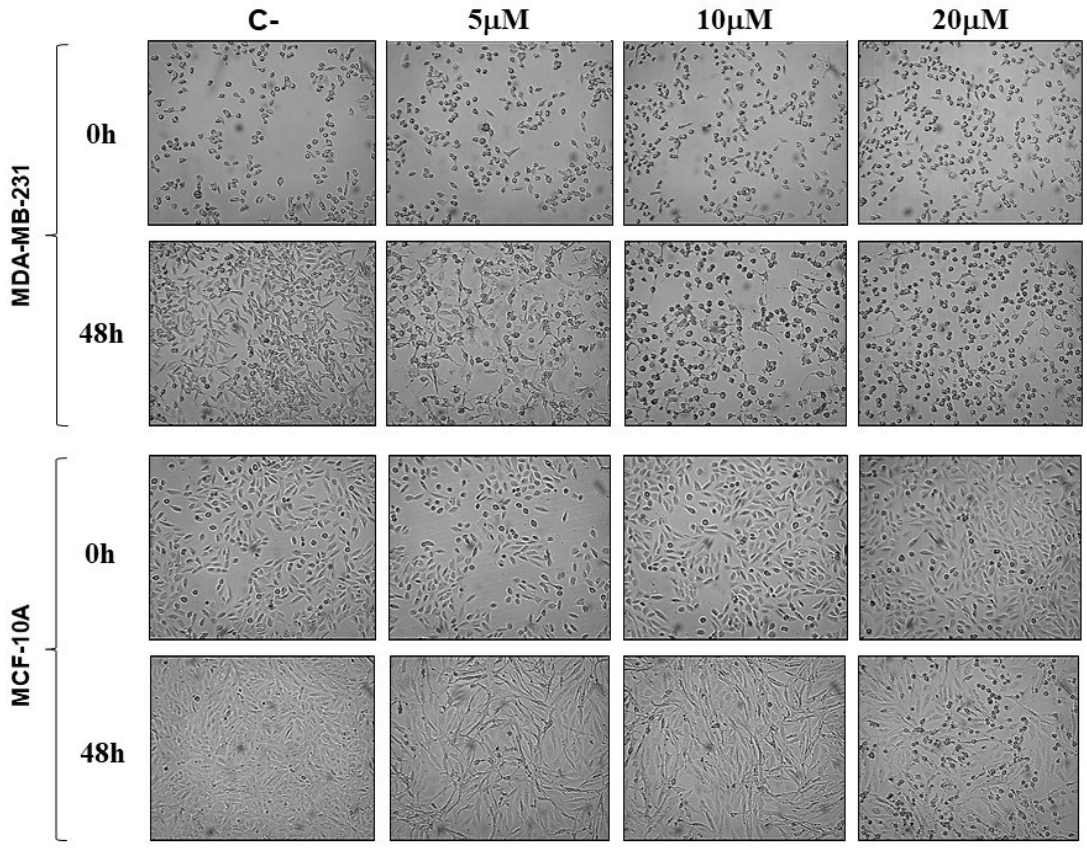

Fig. S11. Morphological changes in MDA-MB-231 and MCF-10A cells incubated with compound **1** for 48 hours. Amplification 10 x.

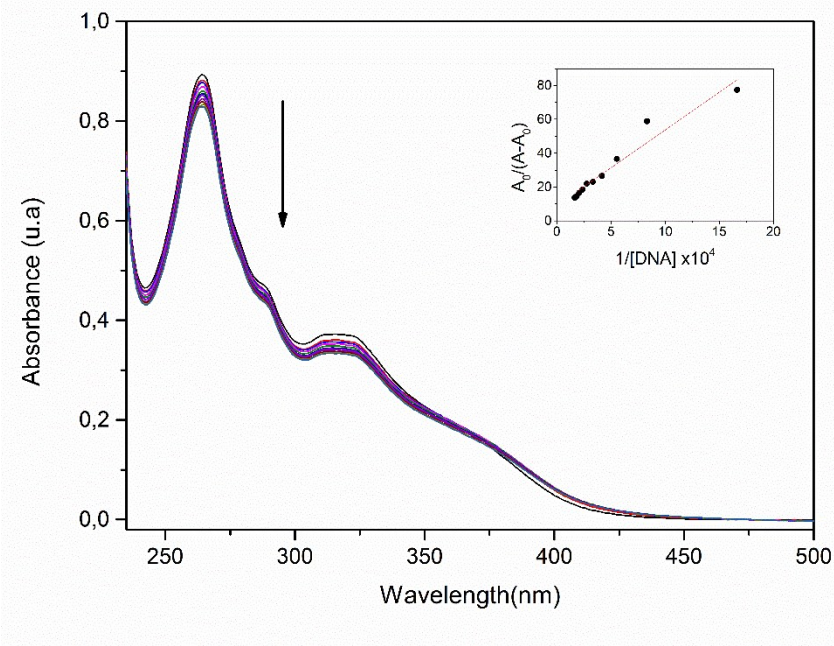

Fig. S12. Absorption titration spectra of compound **1** (20 μM) with increasing amounts of ct-DNA solutions (0 - 60 μM) in Tris-HCl buffer. Inset: plot of 1/[DNA] vs. $A_0/(A-A_0)$.

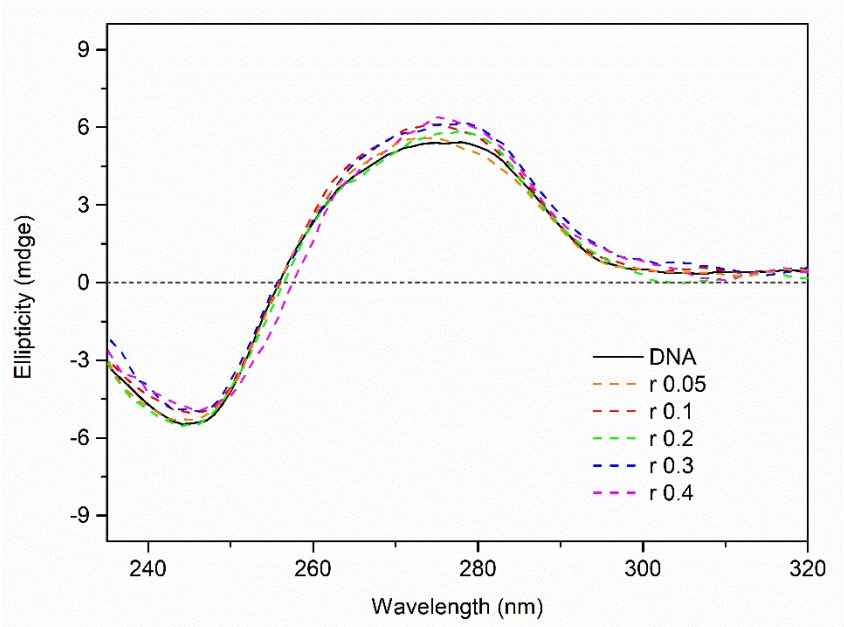

Fig. S13. CD spectrum of ct-DNA in the presence of **1**. r = [complex **1**]/ [DNA].

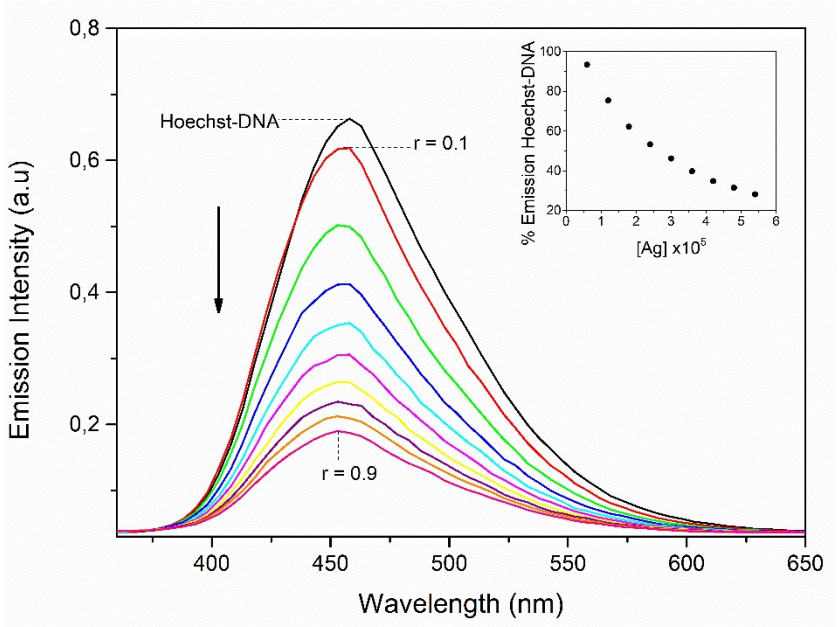

Fig. S14. Emission spectra of Hoechst-bound DNA (λ_{ex} = 350 nm) in the presence of increasing concentrations of **1** (6 - 60 μM) in Tris-HCl buffer. [DNA] = 60 μM; [TO] = 6 μM. Inset: plot [Ag] vs relative emission of Hoechst-bound DNA.

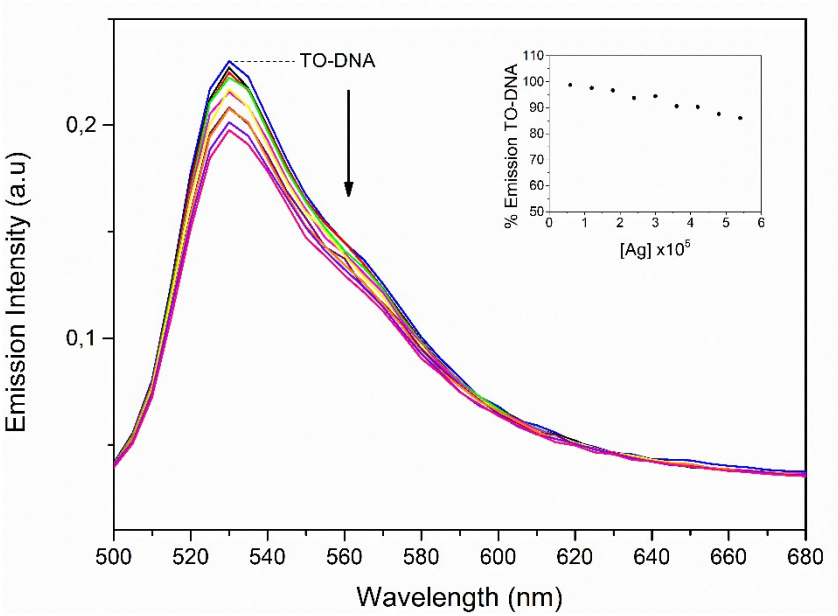

Fig. S15. Emission spectra of TO-bound DNA (λ_{ex} = 480 nm) in the presence of increasing concentrations of **1** (6 - 60 μM) in Tris-HCl buffer. [DNA] = 60 μM; [TO] = 6 μM. Inset: plot [Ag] vs relative emission of TO-bound DNA.

Table S2. Instrumental parameters and temperature program used in the determination of Ag in cell suspension by HR-CS GFAAS.

Wavelength (nm)			328.0683	
Read time (s)			5	
Integration mode of absorbance signal			Area	
Evaluation pixels			3 (CP ± 1)	
Purge gas			Argon	
Gas flow during atomization			Stop	
Working range (pg)			0 – 500	
Step	**Name**	**Temp. (°C)**	**Ramp. (°C s^{-1})**	**Hold (s)**
1	Drying	125	7	30
2	Pyrolysis	800	60	35
3	Gas adaption	800	0	5
4	Atomize	1800	1500	5
5	Clean	2600	1000	3

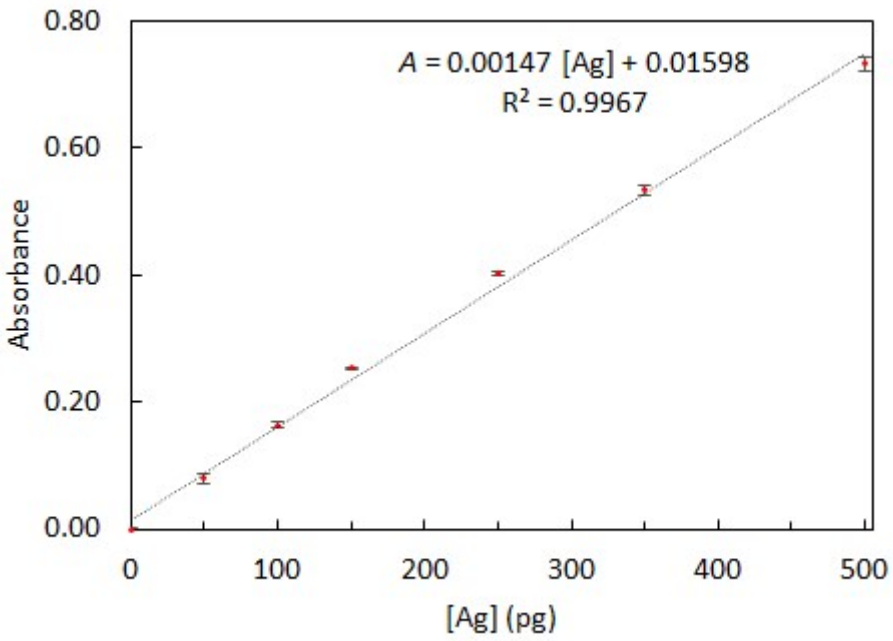

Fig. S16. Calibration curve obtained for Ag determination by HR-CS GFAAS.

Table S3. Percentage of Ag uptake in the cells determined by HR-CS GFAAS (n = 3).

Sample	[Ag] (pg)	Initial concentration (pg)	Uptake percentage (%)
1	714.8 ± 132	6010.7 ± 489.6	11.9
	730.7 ± 170		12.2
	784.6 ± 224		13.1
2	490.6 ± 116	6318.8 ± 168.9	7.8
	497.4 ± 121		7.9
	415.2 ± 35		6.6
3	1991.7 ± 240	9235.2 ± 779.1	21.6
	1841.5 ± 220		19.9
	1139.0 ± 208		12.3